Field microenvironments regulate crop diel transcript and metabolite rhythms

Luíza Lane Barros Dantas[1,2]*, Maíra Marins Dourado[1]*, Natalia Oliveira de Lima[1], Natale Cavaçana[1], Milton Yutaka Nishiyama-Jr.[3], Glaucia Mendes Souza[1], Monalisa Sampaio Carneiro[4], Camila Caldana[5], Carlos Takeshi Hotta[1†]

1 Departamento de Bioquímica, Instituto de Química, Universidade de São Paulo, São Paulo, SP, 05508-000, Brazil

2 Present address: John Innes Centre, Norwich Research Park, Norwich, NR4 7UH, UK

3 Laboratório Especial de Toxicologia Aplicada, Instituto Butantan, São Paulo, SP, 05503-900, Brazil

4 Departamento de Biotecnologia e Produção Vegetal e Animal, Centro de Ciências Agrárias, Universidade Federal de São Carlos, São Carlos, SP, 13600-970, Brazil.

5 Max Planck Institute for Molecular Plant Physiology, Potsdam-Golm, Germany

* These authors contributed equally to the work

† **Correspondence:** Carlos Takeshi Hotta (hotta@iq.usp.br)

Author Contributions: Conceptualization, L.L.B.D., M.S.C., C.T.H.; Methodology, L.L.B.D., C.T.H.; Software, C.T.H., M.Y.N; Validation, L.L.B.D., N.O.L.; Investigation, L.L.B.D., N.O.L., C.T.H., C. C.; Resources, M.S.C., C. C.; Data Curation, C.T.H., M.Y.N; Writing – Original Draft, L.L.B.D., C.T.H.; Writing – Review & Editing, L.L.B.D., M.S.C., C. C., C.T.H.; Visualization; C. T. H.; Project Administration, C. T. H.; Funding Acquisition, C.T.H.

Competing Interests: The authors have no competing interests to declare.

Acknowledgements: This work was supported by the São Paulo Research Foundation (FAPESP) (grant nos. 11/00818-8, 15/06260-0 and 19/08534-0; BIOEN Program) and by the Serrapilheira Institute (grant no. Serra-1708-16001). L. L. B. D. and N. O. L. were supported by FAPESP scholarships (grants 11/08897-4 and 16/06740-4, respectively). We thank the support of Carolina G. Lembke for the oligoarrays hybridization. We thank the support of the LabMET at Brazilian Bioethanol Science and Technology Laboratory (CTBE/CNPEM) for the metabolite profiling analysis (MET-19154 and MET-20673).

Abstract

Most research in plant chronobiology was done in laboratory conditions. However, they usually fail to mimic natural conditions and their nuanced fluctuations, highlighting or obfuscating rhythmicity. High-density crops, such as sugarcane (*Saccharum* hybrid), generate field microenvironments that have specific light and temperature, as they shade each other. Here, we measured the metabolic and transcriptional rhythms in the leaves of 4-month-old (4 mo.) and 9 mo. sugarcane grown in the field. Most of the assayed rhythms in 9 mo. sugarcane peaked >1 h later than in 4 mo. sugarcane, including rhythms of the circadian clock gene, *LATE ELONGATED HYPOCOTYL* (*LHY*), but not *TIMING OF CAB EXPRESSION* (*TOC1*). We hypothesized that older sugarcane perceives dawn later than younger sugarcane, due to self-shading. As a test, we measured *LHY* rhythms in plants on the east and the west side of a field. We also tested if a wooden wall built between lines of sugarcane also changed their rhythms. In both experiments, the *LHY* peak was delayed in the plants shaded at dawn. We conclude that plants in the same field may have different phases due to field microenvironments, which may impact important agronomical traits, such as flowering time, stalk weight and number.

Introduction

Plants are sessile organisms living in constantly changing environments. Some of those changes are rhythmic, due to the movements of the tilted Earth around the Sun, bringing seasons, and around itself, bringing day and night. The circadian oscillator is an adaptation for life in rhythmic environments. It is an internal regulatory network that allows plants to track the time of the day by generating responses on both metabolism and physiology levels. The ability to anticipate the rhythmic changes in the environment increases plants fitness (Green *et al.*, 2002; Dodd *et al.*, 2005). Plants that cannot keep their rhythms, desynchronize with the environment and assimilate less carbon (C), accumulate less biomass and have lower water use efficiency (Dodd *et al.*, 2005). The circadian oscillator network comprises a central oscillator that generates rhythms independently of environmental cues (zeitgebers), such as light and temperature; input pathways that continuously feed the central oscillator with internal and external information, synchronizing it with environmental rhythms (Webb *et al.*, 2019); and output pathways that gather temporal information generated from the interactions between the central oscillator and the input pathways and translate it into timely regulated metabolic and physiologic responses. The plant central oscillator includes several interlocked

feedback loops based on the regulation of transcription and translation. Dawn is marked by an increase in transcripts of *CIRCADIAN CLOCK ASSOCIATED 1* (*CCA1*, not found in monocots), *LATE ELONGATED HYPOCOTYL* (*LHY*) and *REVEILLE 8* (RVE8) expression (Alabadí *et al.*, 2001; Rawat *et al.*, 2011; Gray *et al.*, 2017), which in turn regulate and are regulated by the expression of members of the *PSEUDO RESPONSE REGULATOR* (*PRR*) gene family during the day (Nakamichi *et al.*, 2010; Huang *et al.*, 2012). In monocots, this includes *PRR1*, *PRR37*, *PRR59*, *PRR73*, and *PRR95* (Hotta *et al.*, 2013; Calixto *et al.*, 2015; Dantas *et al.*, 2020). As LHY expression declines during the day, the expression of PRR1, usually called TIMING OF CAB EXPRESSION (TOC1), increases, leading to a peak near dusk (Alabadí *et al.*, 2001). In *Arabidopsis thaliana* (L.) Heynh., TOC1 degradation is regulated by an interplay between ZEITLUPE (AtZTL) and GIGANTEA (AtGI) (Kim *et al.*, 2007; Cha *et al.*, 2017). In eudicots, a protein complex called EVENING COMPLEX (EC), that is composed of LUX ARRHTHMO (LUX), EARLY FLOWERING 3 and 4 (ELF3 and ELF4), is assembled during the night, repressing many other Central Oscillator genes (Herrero *et al.*, 2012). The EC still needs to be confirmed in monocots, even though *ELF3* is present and functional (Zhao *et al.*, 2012; Huang *et al.*, 2017).

Most of the research in plant chronobiology was done in laboratory conditions. However, these conditions usually fail to fully mimic natural conditions and their nuanced fluctuations, highlighting or obfuscating phenomena that could only take place and be observed in the field (Annunziata *et al.*, 2017; Song *et al.*, 2018). In rice (*Oryza sativa* L.), mutations in homolog *OsGI* lead to a delay in flowering in short days and long days in laboratory conditions. However, this phenotype was not observed in long days in the field (Izawa *et al.*, 2011). In *Arabidopsis*, flowering under artificial conditions does not fully mimic flowering in nature due to the light quality and spectra, as well as the temperature gradients found in natural conditions (Song *et al.*, 2018). *Arabidopsis* grown under artificial light also had different metabolic profiles compared to plants grown under natural light (Annunziata *et al.*, 2017). Rhythms in the transcription of plants grown in natural conditions or the field are regulated by the circadian oscillator and by changes in external conditions, such as temperature, light intensity, humidity, and photoperiod, or internal conditions, such as plant age and plant physiology (Nagano *et al.*, 2012, 2019; Matsuzaki *et al.*, 2015; Panter *et al.*, 2019; Dantas *et al.*, 2020).

Here we have measured metabolic and transcriptional rhythms in sugarcane leaves grown in the field. We show that transcript and metabolite rhythms in 4 months old (4 mo.)

sugarcane have earlier peaks in the day compared to 9 mo. sugarcane, with phase shifts ranging from 2 h to 12 h. These phase shifts are correlated with changes in the peak of expression of circadian oscillator genes. Such variation in the timing of the peaks was confirmed by experiments done on plants grown in the east and west sides of the field, or on plants that were separated by a wooden wall. We conclude that the rhythms of metabolites and transcripts associated with the sugarcane circadian oscillator are regulated by external rhythms in field microenvironments.

Results and Discussion

We initially measured metabolite rhythms in commercial sugarcane (*Saccharum* hybrid, cultivar SP80 3280) grown in a field by harvesting the leaves of 4 mo. and 9 mo. sugarcane, at different dates, every 2 h for 26 h, starting 1.5 h before dawn (Figure 1A). All plants were harvested from the middle of the field to avoid margin effects. The metabolic profiles of plants harvested during the day and the night cluster separately, except for the leaves harvested 21 h after dawn (zeitgeber time 21, ZT21) in 4 mo. sugarcane and leaves harvested at ZT01 in 9 mo. sugarcane (Figure 1B). Most of the 20 metabolites that were rhythmic in both plants (75%) peaked later in 9 mo. sugarcane (Figure 1C, Supplemental Figure S2). The largest phase shifts (> 8h), seen in Glutamate, Serine, 5-Oxoproline, Tagatose and GABA (Figure 1G and Supplemental Figures S4I and S5), may be due to differences in plant age. In *Nicotiana tabacum* (L.), a similar phase change was observed in the rhythms of Glutamate and GABA in sink and source leaves (Masclaux-Daubresse *et al.*, 2002).

We also measured rhythms in transcript accumulation using a custom Agilent oligoarrays (Lembke *et al.*, 2012). Transcriptional rhythms of 9 mo. sugarcane leaves were described in previous work, together with transcriptional rhythms of internodes 1&2 and internodes 5 (Dantas *et al.*, 2020). In the transcriptomic analysis of 4 mo. sugarcane leaves, there were 8,553 expressed transcripts, 86% of the expressed transcripts found in 9 mo. sugarcane leaves (9,891) (Figure 2A). We considered that 4,143 of the expressed transcripts were rhythmic in 4 mo. sugarcane leaves (48.4%), lower than in 9 mo. sugarcane leaves (68.3%, Supplemental Figure S6A). About half of the transcripts that were rhythmic in both 4 mo. and 9 mo. sugarcane leaves peaked earlier in the older plants (51.5%), whilst 48,2% peaked within 1 h of each other (Figure 2B).

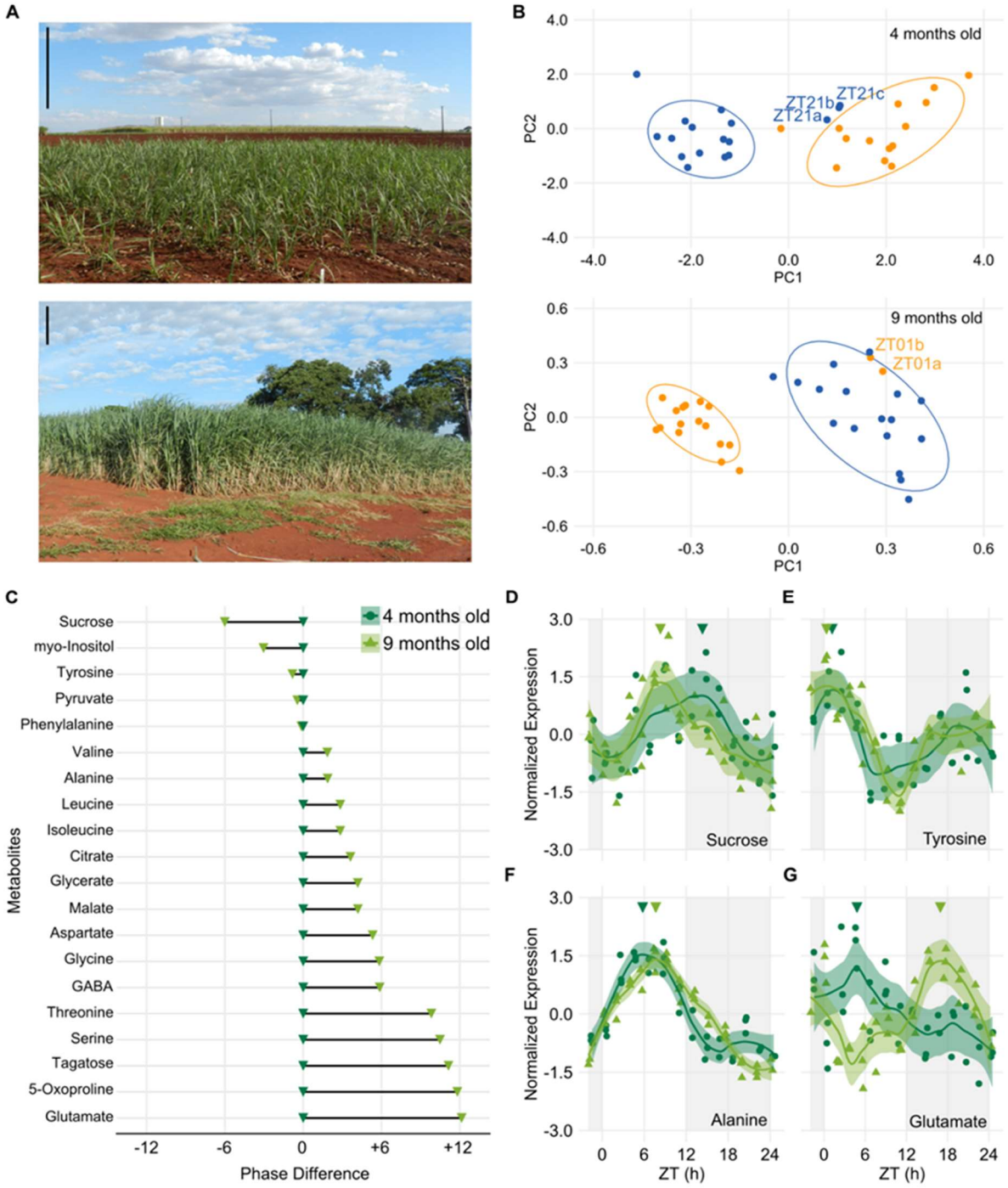

Figure 1. Field-grown sugarcane has metabolic rhythms with different phases. (A) Leaves from sugarcane grown for 4 months old (upper photo) and 9 mo. (lower photo) in the field were harvested for 26 h. Bar = 0.5 m. **(B)** Principal Component Analysis (PCA) of the metabolic data from the leaves of 4 mo. and 9 mo. sugarcane during the day (yellow) or during the night (blue). The percentages of total variance represented by the principal component 1 (PC1) and principal component 2 (PC2) is 63.7% and 60.3%. Metabolites identified in less than 70% of the samples, and samples with less than 70% of the total metabolites identified were excluded from the PCA. Data ellipses were drawn for the samples harvested during the day and the night (0.85 confidence level). **(C)** Phase difference in metabolites that were considered rhythmic in both 4 mo. (dark green) and 9 mo. plants (light green). **(D-G)** Rhythms of **(D)** Sucrose, **(E)** Tyrosine, **(F)** Alanine, and **(G)**

Glutamate in 4 mo. (dark green) and 9 mo. plants (light green). All biological replicates (circles in 4 mo. or triangles in 9 mo.) and their LOESS curve (continuous lines ± SE) are shown. Inverted triangles show the time of the maximum value of the LOESS curve. Metabolite levels were normalized with Z-score. To compare the rhythms of samples harvested in different seasons, the time of harvesting (ZT) was normalized to a photoperiod of 12 h day/ 12 h night. The light-grey boxes represent the night period.

We analyzed the proportion of rhythmic transcripts in different functional categories (Figure 2C and Supplemental Figure 6C). The *Circadian Clock*, *ABA/drought signalling*, *Gibberellin Signalling*, *Transporters*, and *Flowering* are examples of functional categories that have a higher proportion of rhythmic transcripts than the average. Flowering is an important process that could be affected by phase changes in rhythmic genes. As the vegetative stage is the one harvested, flowering is usually undesired in sugarcane. Sugarcane enters the reproductive phase in response to the shortening of the photoperiod over 15 days, and just a 0.5 h difference in photoperiod can trigger flowering in most genotypes (Midmore, 1980; Moore & Berding, 2013; Glassop *et al.*, 2014). Thus, the correct measurement of dawn and dusk is essential for flowering in sugarcane. Several sugarcane genes associated with flowering had their transcription patterns changed. *FLOWERING LOCUS D* (*ScFLD*), a histone acetylase is only expressed in 9 mo. sugarcane leaves, with a peak at ZT9 (Figure 2D). Mutation of *FLD* in Arabidopsis (He *et al.*, 2003) and RNA interference of its homolog in rice(Shibaya *et al.*, 2016) delays flowering. The flowering genes: *CONSTITUTIVE PHOTOMORPHOGENIC 1* (*ScCOP1*) (Tanaka *et al.*, 2011), *CYCLING DOF FACTOR1* (*ScCDF1*)(Higgins *et al.*, 2010), *SHORT VEGETATIVE* (*ScSVP-1* and *-3*) (Higgins *et al.*, 2010), *SUPPRESSOR OF CONSTANS OVEREXPRESSION 1* (*ScSOC1*) (Higgins *et al.*, 2010), *FLOWERING LOCUS T* (Sc*FT*) (Abdul-Awal *et al.*, 2020), and *APETALA* (*ScAP1*)(Preston & Kellogg, 2006) peak an average 2 h earlier in 4 mo. sugarcane leaves, except for *ScSVP-2* (Figure 2E-G and Supplemental Figure 7). Among those genes, *ScSVP*-1, *ScSVP*-3, *ScSOC1*, *ScFT*, and *ScCDF1* peak before dawn in 4 mo. sugarcane leaves and after dawn in 9 mo. sugarcane leaves (2E-G and Supplemental Figure 7A). In Arabidopsis, AtLHY and AtCCA1 reduce AtSVP protein levels, which is a repressor of flowering (Fujiwara *et al.*, 2008). A change in the relative phase between *ScLHY* and *ScSVP* may change the ScSVP protein levels, impacting flowering. Thus, neighbour shading could trigger flowering earlier than the actual critical photoperiod. In sugarcane, photoperiod is perceived by the spindle, a whorl of immature leaves on the top of the plant, which may minimize the effects of shading

177 from neighbour plants (Moore & Berding, 2013; Glassop *et al.*, 2014; Glassop & Rae,
178 2019).

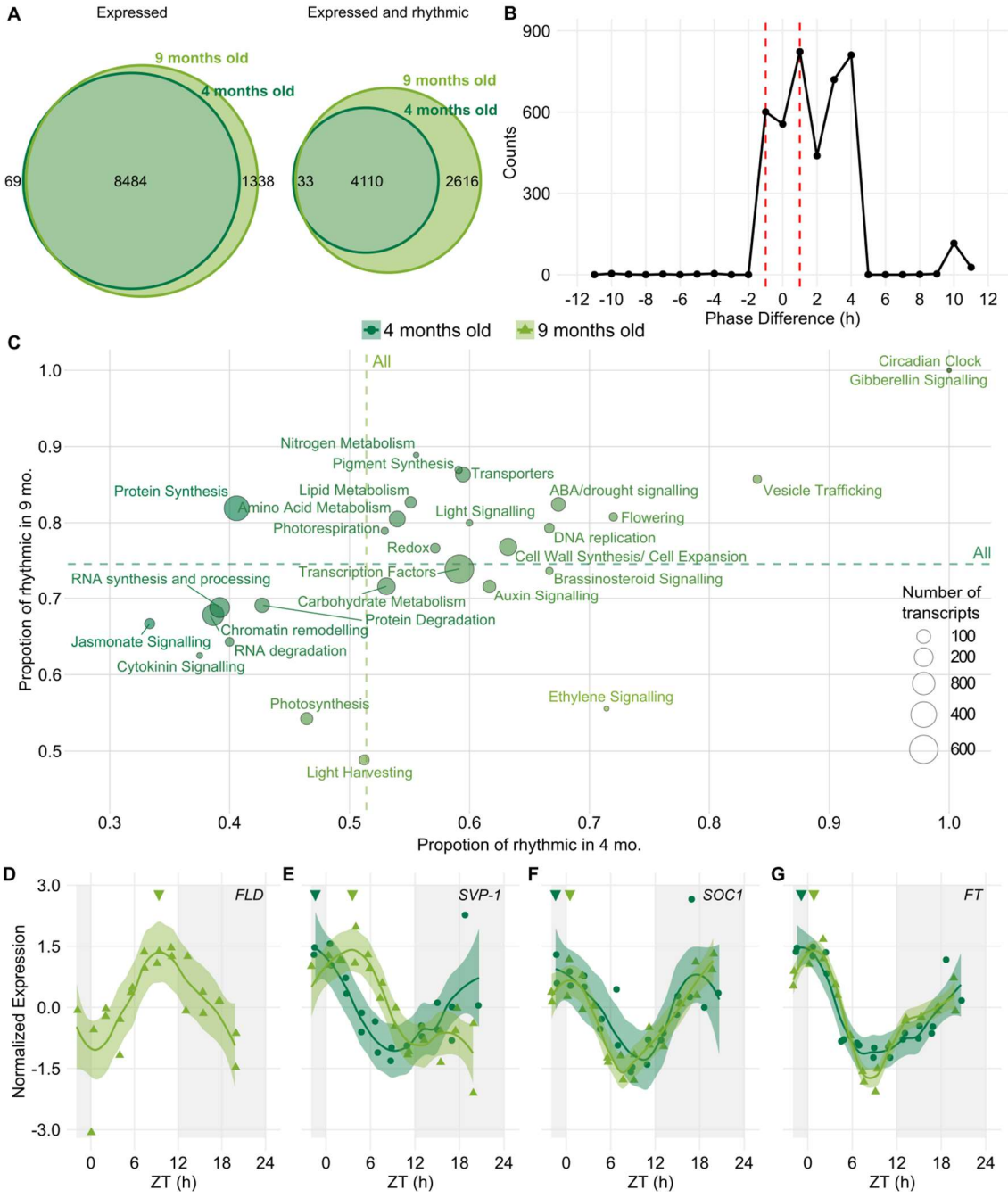

179

180 **Figure 2. Field-grown sugarcane has transcriptional rhythms with different phases.**
181 Leaves from sugarcane grown for 4 months old (4 mo.) and 9 mo. in the field were
182 harvested for 26 h. **(A)** Euler diagrams of all expressed transcripts and expressed
183 transcripts that are rhythmic in 4 mo. (dark green) and 9 mo. (light green) sugarcane
184 leaves in diel conditions. **(B)** Distribution of phase differences between rhythmic
185 transcripts from 4 mo. and 9 mo. sugarcane. Phase differences under ±1 h are not
186 considered significant (red dashed line). **(C)** Proportion of rhythmic transcripts in different
187 functional categories in 4 mo. and 9 mo. sugarcane leaves. The size of the circles shows
188 the total number of expressed transcripts in each category. The colour of the circles

shows if there is an increase in the proportion of rhythmic transcripts in 4 mo. (light green) or in 9 mo. sugarcane leaves (dark green). The dotted lines represent the proportion of rhythmic transcripts among all annotated transcripts. **(D)** *FLOWERING LOCUS D* (*ScFLD*), **(E)** *SHORT VEGETATIVE-1* (*ScSVP*-1), (**F**) *SUPPRESSOR OF CONSTANS OVEREXPRESSION* (*ScSOC1*), and (**G**) *FLOWERING LOCUS T* (*ScFT*) rhythms measured in 4 mo. and 9 mo. sugarcane. All biological replicates and their LOESS curve (continuous lines ± SE) are shown. Inverted triangles show the time of the maximum value of the LOESS curve. Time series were normalized using Z-score. To compare the rhythms of samples harvested in different seasons, the time of harvesting (ZT) was normalized to a photoperiod of 12 h day/ 12 h night. The light-grey boxes represent the night periods.

As the rhythms of metabolites and transcripts were different between 4 mo. and 9 mo. sugarcane leaves, we decided to compare the transcription levels of the core circadian clock genes *ScLHY* and *TIMING OF CAB EXPRESSION* (*ScTOC1*) (Figure 3A and Supplemental Figure S8). As Sc*LHY* peaks at dawn and Sc*TOC1* peaks at dusk under circadian conditions in sugarcane, it is possible to use these genes to track down how the timing of dawn and dusk is perceived by its circadian clock (Hotta *et al.*, 2013). *ScLHY* peaked 0.2 h after dawn in 4 mo. sugarcane leaves but peaked 2.7 h after dawn in 9 mo. sugarcane leaves (Figure 3A and Supplemental Figure S8A). A peak of *LHY* hours after dawn is atypical, as it is light-induced (Mockler *et al.*, 2007). In contrast, *ScTOC1* peaked at 11.0 h and 11.3 h after dawn in 4 mo. and 9 mo. sugarcane leaves, respectively (Figure 3A and Supplemental Figure S8D). Among the other central oscillator genes investigated, *PSEUDO RESPONSE REGULATOR 73* (*ScPRR73*), *ScPRR59*, *ScGI, REVEILLE 8* (*ScRVE8*) and *EARLY FLOWERING 3* (*ScELF3*) also peaked at similar times in 4 mo. and 9 mo. sugarcane leaves, while *ScPRR95* had an earlier peak (-2.6 h) in 9 mo. sugarcane leaves (Supplemental Figure S8). This could explain why only half of the rhythmic genes had phase changes.

A second *ScLHY* peak was also observed starting between 18.0 h and 20.0 h in 4 mo. sugarcane leaves (Figure 3A and Supplemental Figure S8A), also observed in metabolites such as Alanine (Figure 1F) and Pyruvate (Supplemental Figure 3C). A similar night peak was described in *Coffea arabica* L. and attributed to a response to the moonlight (Breitler *et al.*, 2020). In our experiment, the night peak started minutes after the crescent moon was set (ZT17-18).

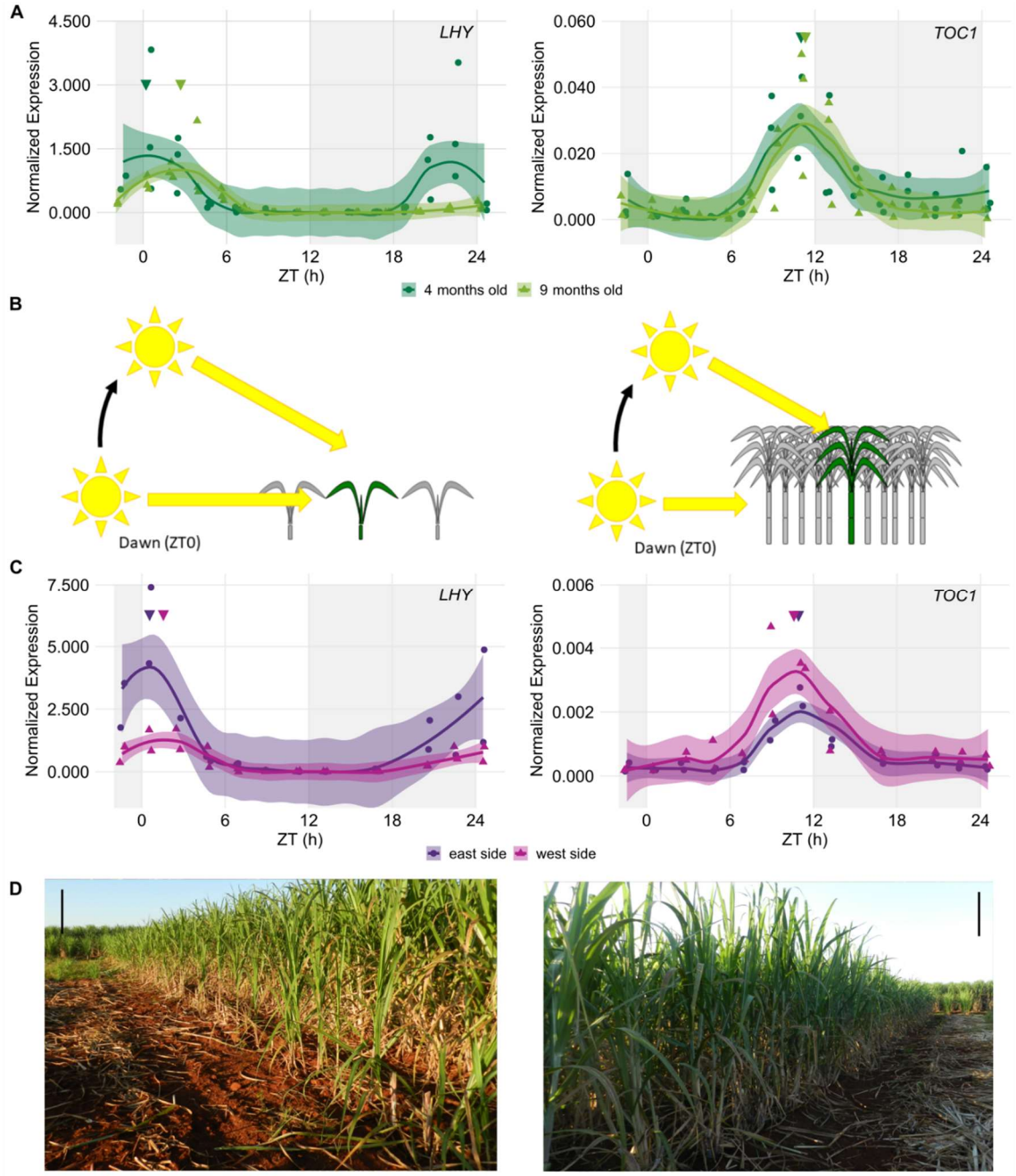

Figure 3. Sugarcane leaves have different ScLHY phases in field-grown sugarcane. Leaves from sugarcane grown for 4 months old (mo.) and 9 mo. in the field were harvested for 26 h. (A) Diel rhythms of LATE ELONGATED HYPOCOTYL (ScLHY) and TIME OF CAB EXPRESSION 1 (ScTOC1) in the leaves of 4 mo. (dark green) and 9 mo. (light green) sugarcane leaves. (B) When sugarcane is 4 months old (left), there is little shading between plants. In comparison, 9 mo. sugarcane shade each other when the sun is at a low angle (right). (C-D) Diel rhythms of ScLHY and ScTOC1 in the leaves of sugarcane grown on the east side (purple, left photo) and the west side (pink, right photo) of the field. Bar = 0.5 m. All biological replicates and their LOESS curve (continuous lines ± SE) are shown. Inverted triangles show the time of the maximum value of the LOESS curve. Time series were normalized using Z-score. To compare the rhythms of samples harvested in different seasons, the time of harvesting (ZT) was normalized to a photoperiod of 12 h day/ 12 h night. The light-grey boxes represent the night periods.

Transcript levels were measured using RT-qPCR. Relative expression was determined using GLYCERALDEHYDE-3-PHOSPHATE DEHYDROGENASE (ScGAPDH).

We hypothesized that phase changes are a consequence of the circadian oscillator of 9 mo. sugarcane perceiving dawn later than 4 mo. sugarcane, as a consequence of shading effects from neighbouring plants. While young sugarcane plants interact little with their neighbours due to their short height, mature sugarcane plants usually grow densely surrounded by other plants and senescent leaves (Figure 1A), shading each other, and making it difficult for low angle sunlight to directly reach leaves uniformly in the entire field (Figure 3B). This hypothesis also explains why the metabolic profile of 9 mo. sugarcane leaves harvested at ZT01, before the *ScLHY* peak, was closer to the leaves harvested during the night than the plants harvested during the day (Figure 1B).

If our hypothesis was correct, plants grow on the east side of a field, that receives direct sunlight at dawn, and the west side would have *ScLHY* rhythms with different phases. Using leaves from 6 mo. plants, we estimated that *ScLHY* from sugarcane peaked 0.6 h after dawn in the east side of the field, and 1 h later on west side (Figure 3C). Light levels were also around 1 h late in the west side of the field in the morning (Figure 3D and Supplemental Figure S1C). These changes could affect the timing of output rhythms, as hundreds of genes are regulated directly by AtLHY in Arabidopsis (Harmer *et al.*, 2000; Adams *et al.*, 2018). In contrast, *ScTOC1* rhythms had similar phases (Figure 3C). In a similar experiment, Grape berries (*Vitis vinifera* L.) harvested from the east and the west side of a vine had different phases in sucrose rhythms(Reshef *et al.*, 2019).

To further confirm our hypothesis, we created artificial shading by building a wooden wall between the first two lines of 5 mo. sugarcane on the east side of the field (Figure 4). The wall was built two days before harvesting to avoid developmental effects, as well as any long-term shade avoidance responses, caused by shading. Plants before the wall received direct sunlight at dawn, while plants after the wall received direct sunlight 0.7 h later (Figure 4A, 4C and Supplemental Figure 1E), which also affected the local temperature (Supplemental Figure 1F). In sugarcane growing before the wall, *ScLHY* expressed in leaves peaked 1.1 h after dawn, whereas *ScLHY* peaked 2.4 h after dawn in leaves that were after the wall (Figure 4B). *ScTOC1* peaked at the same time in both conditions. Combining the three experiments, the peaks of *ScLHY* and *ScTOC1* happened 10.4 ± 0.5 h (n = 3) apart in plants not subjected to shading at dawn and 8.7 ±

0.5 h (n = 3) apart in plants shaded at dawn, which could be enough to trigger photoperiodic responses.

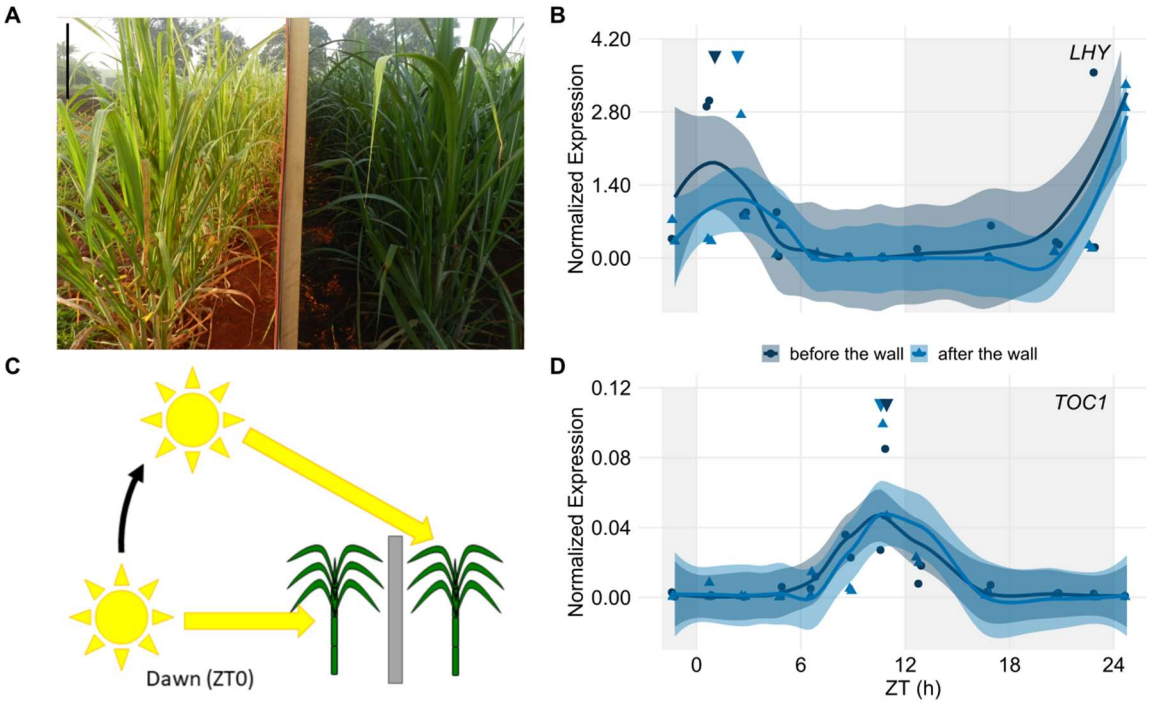

Figure 4. Sugarcane leaves have different *ScLHY* phases on different sides of a wooden wall. (A) Leaves from sugarcane grown before a wooden wall and after the wooden wall were harvested for 26 h. The photo was taken 1 h after dawn and horizontally flipped. Bar = 0.5 m. **(B and D)** Diel rhythms of *LATE ELONGATED HYPOCOTYL* (*ScLHY*) and *TIME OF CAB EXPRESSION 1* (*ScTOC1*) in the leaves of sugarcane grown before the wall (dark blue) and after the wall (light blue). All biological replicates and their LOESS curve (continuous lines ± SE) are shown. Inverted triangles show the time of the maximum value of the LOESS curve. Time series were normalized using Z-score. To compare the rhythms of samples harvested in different seasons, the time of harvesting (ZT) was normalized to a photoperiod of 12 h day/ 12 h night. The light-grey boxes represent the night periods. Transcript levels were measured using RT-qPCR. Relative expression was determined using *GLYCERALDEHYDE-3-PHOSPHATE DEHYDROGENASE* (*ScGAPDH*). **(C)** An artificial wall was used to prevent direct low-angle sunlight to reach sugarcane at dawn.

Microenvironment changes due to shading also affect photosynthesis. In *Arabidopsis*, photosynthetic soluble sugars have been shown to regulate the circadian oscillator (Haydon *et al.*, 2013; Frank *et al.*, 2018). Hence, the phase changes seen in *ScLHY* could be driven by changes in photosynthesis or, specifically, by carbon assimilation into sucrose. Moreover, photosynthesis is one of the factors that impact rhythms in gene expression in *Arabidopsis halleri* subsp. *gemmifera* (Matsum.) O'Kane & Al-Shehbaz in natural conditions (Nagano *et al.*, 2019). It is unclear how the circadian oscillator and

metabolites rhythms are interconnected in sugarcane. However, sucrose and myo-Inositol were the only metabolites that had an earlier phase in the leaves of 9 mo. sugarcane (Figure 1D and Supplemental Figure S3A). Indeed, sucrose levels in the first 4 h of the day were similar in 4 mo. and 9 mo. plants. Hence, sucrose from photosynthesis might not be the factor explaining the observed phase changes, but our analysis only covered a few photosynthetic metabolites.

We found that the location of a plant within a field can change the perception of dawn by the circadian clock due to differences in field microenvironments. The circadian clock regulates carbon allocation, which may impact agronomic traits (Yazdanbakhsh *et al.*, 2011; Kölling *et al.*, 2015). In *Sorghum bicolor* (L.) Moench. grown at high and low densities, changes in transcription levels of *SbLHY* and *SbTOC1* were correlated with differences in internode length (Kebrom *et al.*, 2020). As only one time point was sampled in that study, the detected differences in expression levels could be an indication of the phase differences we detected (Supplemental Figure S9). When row spacings in sugarcane fields were changed between 1.5 m and 2.3 m, cane yields (t/ha) were maintained, as the stalk numbers and weight would change in response to different plant densities (Garside *et al.*, 2009; Chiluwal *et al.*, 2018). In grapes,

The circadian clock increases the productivity of plants when its phase matches the phase of environmental rhythms (Dodd *et al.*, 2005). It is usually accepted that rhythms of plants under the same photoperiod have matching phases. We have evidence that field microenvironmental rhythms and not astronomical rhythms regulate the plant circadian oscillator of plants in natural, fluctuating conditions, as well as transcriptional and metabolic rhythms. Rhythms in field microenvironments are another factor to consider when translating knowledge from the lab to the field.

Materials and Methods

Field conditions, plant growth, and harvesting

All three assayed sugarcane fields were located in the same area, at the Federal University of São Carlos, campus Araras, in São Paulo state, Brazil (22°21′25″ S, 47°23′3″ W; altitude of 611 m). The soil was classified as a Typic Eutroferric Red Latosol. Sugarcane from the commercial variety SP80 3280 (*Saccharum* hybrid) was used in all experiments. The environmental conditions for the three experiments were collected from a local weather station or from within the field (Supplemental Figure S1). Light intensity

was measured with the sensor parallel to the ground. Plants were sampled every 2 h for 26 h, starting 1.5 h before dawn. For all experiments, the leaves +1 of nine sugarcane individuals were harvested and separated into three pools of three individuals, each pool was considered a biological replicate. The leaves +1 are the first fully photosynthetically active leaf in sugarcane. Each sampling took less than 30 min and the harvested tissue was immediately frozen in liquid nitrogen. In the first experiment, sugarcane was planted in April/2012 and sampled in August/2012 (4 months old), during winter, and in January/2013 (9 months old), during summer. In winter, dawn was at 6:30, and dusk was at 18:00 (11.5 h day/12.5 h night). In summer, dawn was at 5:45, and dusk was at 19:00 (13.25 h day/10.75 h night). For the second experiment (east and west margins), plants were planted in October/2014 and harvested in March/2015 (5 months old) (12.0 h day/12.0 h night). In the third experiment, plants (the wall experiment) were also planted in October/2014, but harvested in April/2015 (6 months old) (11.25 h day/12.75 h night). The orientation of the sugarcane was north to south. In the wall experiment, a 2 m high wall made of plywood sheets was built between the first and the second rows on the east side of the field two days before harvest day. To compare the rhythms of samples harvested in different seasons, the time of harvesting was normalized to a photoperiod of 12 h day/ 12 h night using the following equations: for times during the daytime, ZT = 12*T*Pd-1, where ZT is the normalized time, T is the time from dawn (in hours), and Pd is the length of the day (in hours); for times during the nighttime, ZT = 12 + 12*(T - Pd)*Pn-1, where ZT is the normalized time, T is the time from dawn (in hours), Pd is the length of the day (in hours), and Pn is the length of the night (in hours).

Metabolome

Metabolites were extracted from all 3 biological replicates. 50 mg of the grounded tissue was used for MTBE: methanol: water 3:1:1 (v/v/v) extraction, as described previously (Giavalisco *et al.*, 2011). The 100 µl of the organic phase was dried and derivatized as previously described (Roessner *et al.*, 2001). 1 µl of the derivatized samples were analyzed on a Combi-PAL autosampler (Agilent Technologies) coupled to an Agilent 7890 gas chromatograph coupled to a Leco Pegasus 2 time-of-flight mass spectrometer (LECO, St. Joseph, MI, USA) in both split (1:40) and splitless modes (Weckwerth *et al.*, 2004; Ferreira *et al.*, 2018). Chromatograms were exported from Leco ChromaTOF software (version 3.25) to R software. Peak detection, retention time alignment, and library matching were performed using *Target Search R-package* (Cuadros-Inostroza *et*

al., 2009). Metabolites were quantified by the peak intensity of a selective mass. Metabolites intensities were normalized by dividing the fresh-weight, followed by the sum of total ion count and global outlier replacement as described previously (Giavalisco *et al.*, 2011). Each metabolite value was further normalized to Z-score. The principal component analysis was performed using *pcaMethods* Bioconductor R package. Data ellipses were drawn for the samples harvested during the day and the night (0.85 confidence level).

Oligoarray hybridizations

Oligoarrays were hybridized as described before (Hotta *et al.*, 2013; Dantas *et al.*, 2020). Briefly, frozen samples were pulverized in dry, and 100 mg were used for total RNA extraction using Trizol (Life Technologies). The RNA was treated with DNase I (Life Technologies) and cleaned using the RNeasy Plant Mini kit (Qiagen) following the supplier´s recommendations. The total RNA quality was assayed using an Agilent RNA 6000 Nano Kit Bioanalyzer chip (Agilent Technologies). Labelling was done following the Low Input Quick Amp Labelling protocol of the Two-Color Microarray-Based Gene Expression Analysis system (Agilent Technologies). Hybridizations were done using a custom 4×44 k oligoarray (Agilent Technologies) that was previously described (Lembke *et al.*, 2012; Hotta *et al.*, 2013). Two hybridizations were done for each time point against an equimolar pool of all samples of each organ. Each duplicate was prepared independently using dye swaps. Data were extracted using the Feature Extraction software (Agilent Technologies). Background correction was applied to each dataset. A nonlinear LOWESS normalization was also applied to the datasets to minimize variations due to experimental manipulation. Signals that were distinguishable from the local background signal were taken as an indication that the corresponding transcript was expressed. The GenBank IDs of all sugarcane genes mentioned here can be found in the Supplemental Material (Supplemental Table S1). The complete dataset can be found at the Gene Expression Omnibus public database under the accession number GSE129543 and GSE171222.

Data analysis

For further analysis, only transcripts that were found to be expressed in more than 6 of the 12 time points were considered to be expressed. Identification of rhythmic transcripts was

done using an algorithm described in a previous work (Dantas *et al.*, 2020). All the time series from expressed transcripts were grouped in co-expressed modules using the R package weighted correlation network analysis (WGCNA) (Langfelder & Horvath, 2008) with the same parameters as before (Dantas *et al.*, 2020). Co-expression modules were considered rhythmic or non-rhythmic using JTK-CYCLE (*P*-value of < 0.75) (Hughes *et al.*, 2010). LOESS (locally estimated scatterplot smoothing) regression was used to establish the timing of the peak, or the phase, of each rhythmic time series (Dantas *et al.*, 2019). Euler diagrams were done using the R package *eulerr*. Code to fully reproduce our analysis is available on GitHub (https://github.com/LabHotta/Microenvironments) and archived on Zenodo (http://doi.org/10.5281/zenodo.4645464).

RT-qPCR analysis

Frozen leaf samples were pulverized on dry ice using a coffee grinder (Model DCG-20, Cuisinart, China). 100 mg of each pulverized samples were used for total RNA extractions using Trizol (Life Technologies), according to the manufacturer's protocol. Total RNA was treated with DNase I (Life Technologies) and cleansed using the RNeasy Plant Mini Kit (Qiagen). Both RNA quality and concentration were checked using Agilent RNA 6000 Nano Kit Bioanalyzer chip (Agilent Technologies). 5 µg of the purified RNA was used in the reverse transcription reactions using the SuperScript III First-Strand Synthesis System for RT-PCR (Life Technologies). The RT-qPCR reactions were done using Power SYBR Green PCR Master Mix (Applied Biosystems), 10× diluted cDNA, and specific primers as previously described (Hotta *et al.*, 2013). Reactions were placed in 96-well plates and read with the Fast 7500/7500 Real-Time PCR System (Applied Biosystems). Ct determination was performed using the Fast 7500/7500 Real-Time PCR System built-in software (Applied Biosystems). The $2^{-\Delta CT}$ method was used to calculate relative expression, using *GLYCERALDEHYDE-3-PHOSPHATE DEHYDROGENASE* (*ScGAPDH*) as a reference gene (Hotta *et al.*, 2013). All primers used can be found in the Supplemental Material (Supplemental Table S2).

References

Abdul-Awal SM, Chen J, Xin Z, Harmon FG. **2020**. A sorghum gigantea mutant attenuates florigen gene expression and delays flowering time. *Plant Direct* **4**: e00281.

Adams S, Grundy J, Veflingstad SR, Dyer NP, Hannah MA, Ott S, Carré IA. **2018**. Circadian control of abscisic acid biosynthesis and signalling pathways revealed by genome-wide analysis of LHY binding targets. *New Phytologist* **220**: 893–907.

Alabadí D, Oyama T, Yanovsky MJ, Harmon FG, Más P, Kay SA. **2001**. Reciprocal regulation between TOC1 and LHY/CCA1 within the Arabidopsis circadian clock. *Science (New York, N.Y.)* **293**: 880–883.

Annunziata MG, Apelt F, Carillo P, Krause U, Feil R, Mengin V, Lauxmann MA, Köhl K, Nikoloski Z, Stitt M, *et al.* 2017. Getting back to nature: a reality check for experiments in controlled environments. *Journal of Experimental Botany* **68**: 4463–4477.

Breitler J-C, Djerrab D, Leran S, Toniutti L, Guittin C, Severac D, Pratlong M, Dereeper A, Etienne H, Bertrand B. **2020**. Full moonlight-induced circadian clock entrainment in Coffea arabica. *BMC Plant Biology* **20**: 24.

Calixto CPG, Waugh R, Brown JWS. **2015**. Evolutionary relationships among barley and Arabidopsis core circadian clock and clock-associated genes. *Journal of Molecular Evolution* **80**: 108–119.

Cha J-Y, Kim J, Kim T-S, Zeng Q, Wang L, Lee SY, Kim W-Y, Somers DE. **2017**. GIGANTEA is a co-chaperone which facilitates maturation of ZEITLUPE in the Arabidopsis circadian clock. *Nature Communications* **8**: 3.

Chiluwal A, Singh HP, Sainju U, Khanal B, Whitehead WF, Singh BP. **2018**. Spacing Effect on Energy Cane Growth, Physiology, and Biomass Yield. *Crop Science* **58**: 1371–1384.

Cuadros-Inostroza A, Caldana C, Redestig H, Kusano M, Lisec J, Peña-Cortés H, Willmitzer L, Hannah MA. **2009**. TargetSearch--a Bioconductor package for the efficient preprocessing of GC-MS metabolite profiling data. *BMC bioinformatics* **10**: 428.

Dantas LL de B, Almeida-Jesus FM, de Lima NO, Alves-Lima C, Nishiyama-Jr MY, Carneiro MS, Souza GM, Hotta CT. **2020**. Rhythms of Transcription in Field-Grown Sugarcane Are Highly Organ Specific. *Scientific Reports* **10**: 6565.

Dantas LLB, Calixto CPG, Dourado MM, Carneiro MS, Brown JWS, Hotta CT. **2019**. Alternative Splicing of Circadian Clock Genes Correlates With Temperature in Field-Grown Sugarcane. *Frontiers in Plant Science* **10**.

Dodd AN, Salathia N, Hall A, Kevei E, Toth R, Nagy F, Hibberd JM, Millar AJ, Webb AA. **2005**. Plant circadian clocks increase photosynthesis, growth, survival, and competitive advantage. *Science* **309**: 630–3.

Ferreira DA, Martins MCM, Cheavegatti-Gianotto A, Carneiro MS, Amadeu RR, Aricetti JA, Wolf LD, Hoffmann HP, de Abreu LGF, Caldana C. **2018**. Metabolite Profiles of Sugarcane Culm Reveal

459 the Relationship Among Metabolism and Axillary Bud Outgrowth in Genetically Related Sugarcane
460 Commercial Cultivars. *Frontiers in Plant Science* **9**.

461 **Frank A, Matiolli CC, Viana AJC, Hearn TJ, Kusakina J, Belbin FE, Wells Newman D, Yochikawa A,**
462 **Cano-Ramirez DL, Chembath A, *et al.* 2018**. Circadian entrainment in Arabidopsis by the sugar-
463 responsive transcription factor bZIP63. *Current Biology* **28**: 2597-2606.e6.

464 **Fujiwara S, Oda A, Yoshida R, Niinuma K, Miyata K, Tomozoe Y, Tajima T, Nakagawa M, Hayashi**
465 **K, Coupland G, *et al.* 2008**. Circadian Clock Proteins LHY and CCA1 Regulate SVP Protein
466 Accumulation to Control Flowering in Arabidopsis. *The Plant Cell* **20**: 2960–2971.

467 **Garside AL, Bell MJ, Robotham BG, Garside AL, Bell MJ, Robotham BG**. **2009**. Row spacing and
468 planting density effects on the growth and yield of sugarcane. 2. Strategies for the adoption of
469 controlled traffic. *Crop and Pasture Science* **60**: 544–554.

470 **Giavalisco P, Li Y, Matthes A, Eckhardt A, Hubberten H-M, Hesse H, Segu S, Hummel J, Köhl K,**
471 **Willmitzer L**. **2011**. Elemental formula annotation of polar and lipophilic metabolites using (13) C,
472 (15) N and (34) S isotope labelling, in combination with high-resolution mass spectrometry. *The*
473 *Plant Journal: For Cell and Molecular Biology* **68**: 364–376.

474 **Glassop D, Rae AL**. **2019**. Expression of sugarcane genes associated with perception of
475 photoperiod and floral induction reveals cycling over a 24-hour period. *Functional Plant Biology*
476 **46**: 314–327.

477 **Glassop D, Rae AL, Bonnett GD**. **2014**. Sugarcane Flowering Genes and Pathways in Relation to
478 Vegetative Regression. *Sugar Tech* **16**: 235–240.

479 **Gray JA, Shalit-Kaneh A, Chu DN, Hsu PY, Harmer SL**. **2017**. The REVEILLE Clock Genes Inhibit
480 Growth of Juvenile and Adult Plants by Control of Cell Size. *Plant Physiology* **173**: 2308–2322.

481 **Green RM, Tingay S, Wang Z-Y, Tobin EM**. **2002**. Circadian rhythms confer a higher level of fitness
482 to Arabidopsis plants. *Plant Physiology* **129**: 576–584.

483 **Harmer SL, Hogenesch JB, Straume M, Chang HS, Han B, Zhu T, Wang X, Kreps JA, Kay SA**. **2000**.
484 Orchestrated transcription of key pathways in Arabidopsis by the circadian clock. *Science (New*
485 *York, N.Y.)* **290**: 2110–2113.

486 **Haydon MJ, Mielczarek O, Robertson FC, Hubbard KE, Webb AA**. **2013**. Photosynthetic
487 entrainment of the Arabidopsis thaliana circadian clock. *Nature* **502**: 689–92.

488 **He Y, Michaels SD, Amasino RM**. **2003**. Regulation of flowering time by histone acetylation in
489 Arabidopsis. *Science (New York, N.Y.)* **302**: 1751–1754.

490 **Herrero E, Kolmos E, Bujdoso N, Yuan Y, Wang M, Berns MC, Uhlworm H, Coupland G, Saini R,**
491 **Jaskolski M, *et al.* 2012**. EARLY FLOWERING4 recruitment of EARLY FLOWERING3 in the nucleus
492 sustains the Arabidopsis circadian clock. *The Plant Cell* **24**: 428–443.

493 **Higgins JA, Bailey PC, Laurie DA**. **2010**. Comparative Genomics of Flowering Time Pathways Using
494 Brachypodium distachyon as a Model for the Temperate Grasses. *PLOS ONE* **5**: e10065.

Hotta CT, Nishiyama MY, Souza GM. **2013**. Circadian rhythms of sense and antisense transcription in sugarcane, a highly polyploid crop. *PLoS One* **8**: e71847.

Huang H, Gehan MA, Huss SE, Alvarez S, Lizarraga C, Gruebbling EL, Gierer J, Naldrett MJ, Bindbeutel RK, Evans BS, *et al.* 2017. Cross-species complementation reveals conserved functions for EARLY FLOWERING 3 between monocots and dicots. *Plant Direct* **1**: e00018.

Huang W, Pérez-García P, Pokhilko A, Millar AJ, Antoshechkin I, Riechmann JL, Mas P. **2012**. Mapping the Core of the Arabidopsis Circadian Clock Defines the Network Structure of the Oscillator. *Science* **336**: 75–79.

Hughes ME, Hogenesch JB, Kornacker K. **2010**. JTK_CYCLE: an efficient nonparametric algorithm for detecting rhythmic components in genome-scale data sets. *Journal of Biological Rhythms* **25**: 372–380.

Izawa T, Mihara M, Suzuki Y, Gupta M, Itoh H, Nagano AJ, Motoyama R, Sawada Y, Yano M, Hirai MY, *et al.* 2011. Os-GIGANTEA confers robust diurnal rhythms on the global transcriptome of rice in the field. *The Plant Cell* **23**: 1741–1755.

Kebrom TH, McKinley BA, Mullet JE. **2020**. Shade signals alter the expression of circadian clock genes in newly-formed bioenergy sorghum internodes. *Plant Direct* **4**: e00235.

Kim W-Y, Fujiwara S, Suh S-S, Kim J, Kim Y, Han L, David K, Putterill J, Nam HG, Somers DE. **2007**. ZEITLUPE is a circadian photoreceptor stabilized by GIGANTEA in blue light. *Nature* **449**: 356–360.

Kölling K, Thalmann M, Müller A, Jenny C, Zeeman SC. **2015**. Carbon partitioning in Arabidopsis thaliana is a dynamic process controlled by the plants metabolic status and its circadian clock. *Plant, Cell & Environment* **38**: 1965–1979.

Langfelder P, Horvath S. **2008**. WGCNA: an R package for weighted correlation network analysis. *BMC bioinformatics* **9**: 559.

Lembke CG, Nishiyama MY, Sato PM, de Andrade RF, Souza GM. **2012**. Identification of sense and antisense transcripts regulated by drought in sugarcane. *Plant Molecular Biology* **79**: 461–477.

Masclaux-Daubresse C, Valadier M-H, Carrayol E, Reisdorf-Cren M, Hirel B. **2002**. Diurnal changes in the expression of glutamate dehydrogenase and nitrate reductase are involved in the C/N balance of tobacco source leaves. *Plant, Cell & Environment* **25**: 1451–1462.

Matsuzaki J, Kawahara Y, Izawa T. **2015**. Punctual transcriptional regulation by the rice circadian clock under fluctuating field conditions. *The Plant Cell* **27**: 633–648.

Midmore DJ. **1980**. Effects of photoperiod on flowering and fertility of sugarcane (Saccharum spp.). *Field Crops Research* **3**: 65–81.

Mockler TC, Michael TP, Priest HD, Shen R, Sullivan CM, Givan SA, McEntee C, Kay SA, Chory J. **2007**. The DIURNAL project: DIURNAL and circadian expression profiling, model-based pattern matching, and promoter analysis. *Cold Spring Harbor Symposia on Quantitative Biology* **72**: 353–363.

Moore PH, Berding N. **2013**. Flowering. In: Sugarcane: Physiology, Biochemistry, and Functional Biology. John Wiley & Sons, Ltd, 379–410.

Nagano AJ, Kawagoe T, Sugisaka J, Honjo MN, Iwayama K, Kudoh H. **2019**. Annual transcriptome dynamics in natural environments reveals plant seasonal adaptation. *Nature Plants* **5**: 74.

Nagano AJ, Sato Y, Mihara M, Antonio BA, Motoyama R, Itoh H, Nagamura Y, Izawa T. **2012**. Deciphering and prediction of transcriptome dynamics under fluctuating field conditions. *Cell* **151**: 1358–1369.

Nakamichi N, Kiba T, Henriques R, Mizuno T, Chua N-H, Sakakibara H. **2010**. PSEUDO-RESPONSE REGULATORS 9, 7, and 5 are transcriptional repressors in the Arabidopsis circadian clock. *The Plant Cell* **22**: 594–605.

Panter PE, Muranaka T, Cuitun-Coronado D, Graham CA, Yochikawa A, Kudoh H, Dodd AN. **2019**. Circadian Regulation of the Plant Transcriptome Under Natural Conditions. *Frontiers in Genetics* **10**.

Preston JC, Kellogg EA. **2006**. Reconstructing the Evolutionary History of Paralogous APETALA1/FRUITFULL-Like Genes in Grasses (Poaceae). *Genetics* **174**: 421–437.

Rawat R, Takahashi N, Hsu PY, Jones MA, Schwartz J, Salemi MR, Phinney BS, Harmer SL. **2011**. REVEILLE8 and PSEUDO-REPONSE REGULATOR5 form a negative feedback loop within the Arabidopsis circadian clock. *PLoS genetics* **7**: e1001350.

Reshef N, Fait A, Agam N. **2019**. Grape berry position affects the diurnal dynamics of its metabolic profile. *Plant, Cell & Environment* **42**: 1897–1912.

Roessner U, Luedemann A, Brust D, Fiehn O, Linke T, Willmitzer L, Fernie A. **2001**. Metabolic profiling allows comprehensive phenotyping of genetically or environmentally modified plant systems. *The Plant Cell* **13**: 11–29.

Shibaya T, Hori K, Ogiso-Tanaka E, Yamanouchi U, Shu K, Kitazawa N, Shomura A, Ando T, Ebana K, Wu J, *et al.* 2016. Hd18, Encoding Histone Acetylase Related to Arabidopsis FLOWERING LOCUS D, is Involved in the Control of Flowering Time in Rice. *Plant & Cell Physiology* **57**: 1828–1838.

Song YH, Kubota A, Kwon MS, Covington MF, Lee N, Taagen ER, Laboy Cintrón D, Hwang DY, Akiyama R, Hodge SK, *et al.* 2018. Molecular basis of flowering under natural long-day conditions in Arabidopsis. *Nature Plants* **4**: 824–835.

Tanaka N, Itoh H, Sentoku N, Kojima M, Sakakibara H, Izawa T, Itoh J-I, Nagato Y. **2011**. The COP1 Ortholog PPS Regulates the Juvenile–Adult and Vegetative–Reproductive Phase Changes in Rice. *The Plant Cell* **23**: 2143–2154.

Webb AAR, Seki M, Satake A, Caldana C. **2019**. Continuous dynamic adjustment of the plant circadian oscillator. *Nature Communications* **10**: 550.

Weckwerth W, Wenzel K, Fiehn O. **2004**. Process for the integrated extraction, identification and quantification of metabolites, proteins and RNA to reveal their co-regulation in biochemical networks. *Proteomics* **4**: 78–83.

569 **Yazdanbakhsh N, Sulpice R, Graf A, Stitt M, Fisahn J**. **2011**. Circadian control of root elongation
570 and C partitioning in Arabidopsis thaliana. *Plant, Cell & Environment* **34**: 877–894.

571 **Zhao J, Huang X, Ouyang X, Chen W, Du A, Zhu L, Wang S, Deng XW, Li S**. **2012**. OsELF3-1, an
572 Ortholog of Arabidopsis EARLY FLOWERING 3, Regulates Rice Circadian Rhythm and Photoperiodic
573 Flowering. *PLOS ONE* **7**: e43705.

574

575 **Supplemental Figure 1**

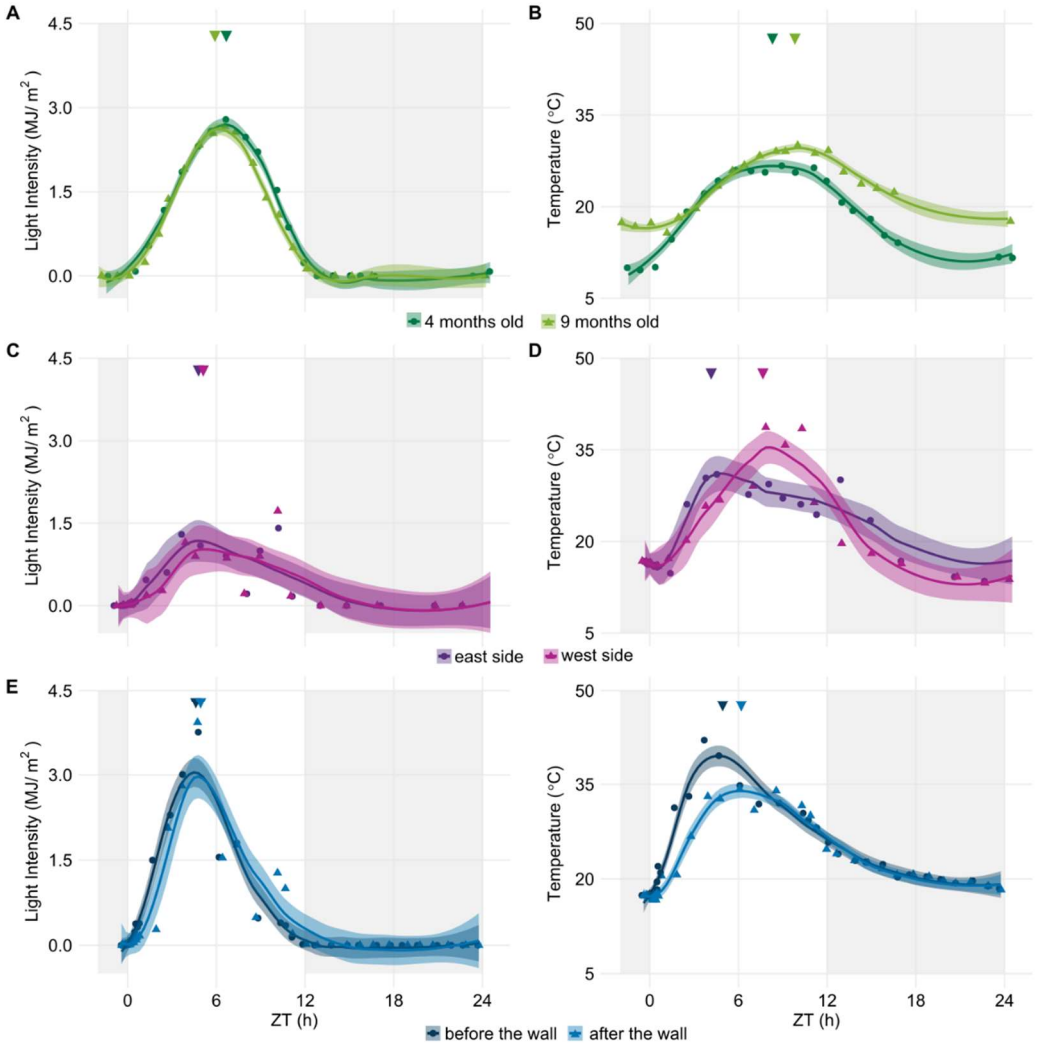

576

577 **Figure S1 – Environmental conditions in Araras (SP, Brazil. (A)** Light intensity and **(B)**
578 temperature on the day of harvesting 4 months old (4 mo.) (green) and 9 mo. (light green)
579 sugarcane. Data was taken from a meteorological station nearby the sugarcane field. **(C)**
580 Light intensity and **(D)** temperature on the day of harvesting 6 mo. sugarcane in the east
581 (purple) or the west side (pink) of the field. Data was taken from sensors installed next to
582 the plants. **(E)** Light intensity and **(F)** temperature on the day of harvesting 5 mo.
583 sugarcane in the east side of the field (dark blue) and sugarcane that were shaded by an
584 artificial wall (light blue). Data was taken from sensors installed next to the plants. All data
585 and their LOESS curve (continuous lines ± SE) are shown. Inverted triangles show the
586 time of the maximum value of the LOESS curve. To compare the rhythms of samples
587 harvested in different seasons, the time of harvesting (ZT) was normalized to a
588 photoperiod of 12 h day/ 12 h night. The light-grey boxes represent the night period.

589 **Supplemental Figure 2**

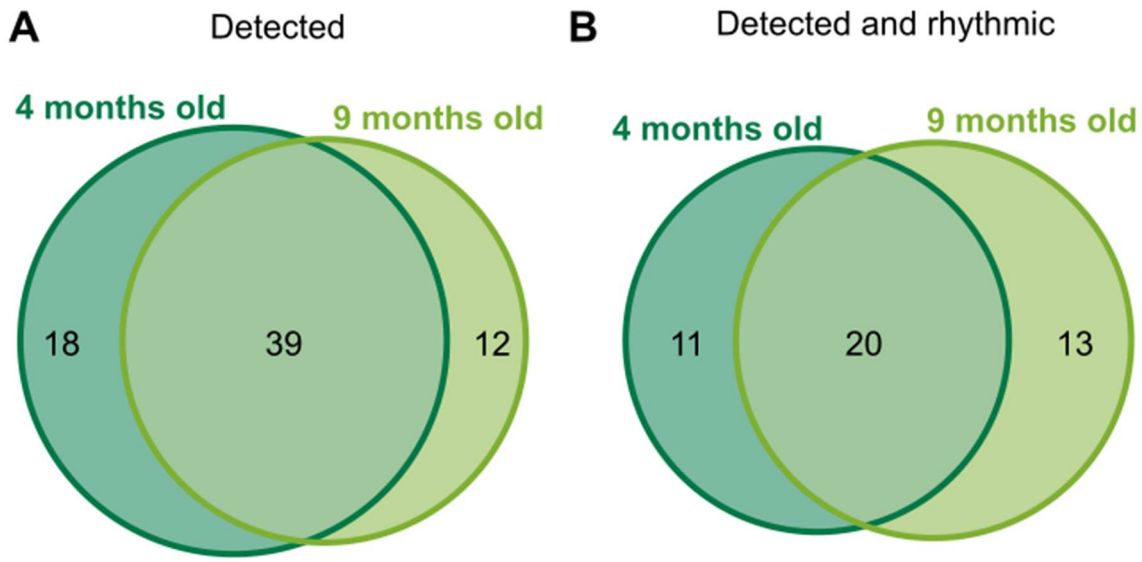

590

591 **Figure S2 – Euler diagram of detected and rhythmic metabolites.** Euler diagrams of
592 all **(A)** detected metabolites and **(B)** rhythmic metabolites in 4 mo. (dark green) and 9 mo.
593 (light green) sugarcane leaves in diel conditions.

594

595

596 **Supplemental Figure 3**

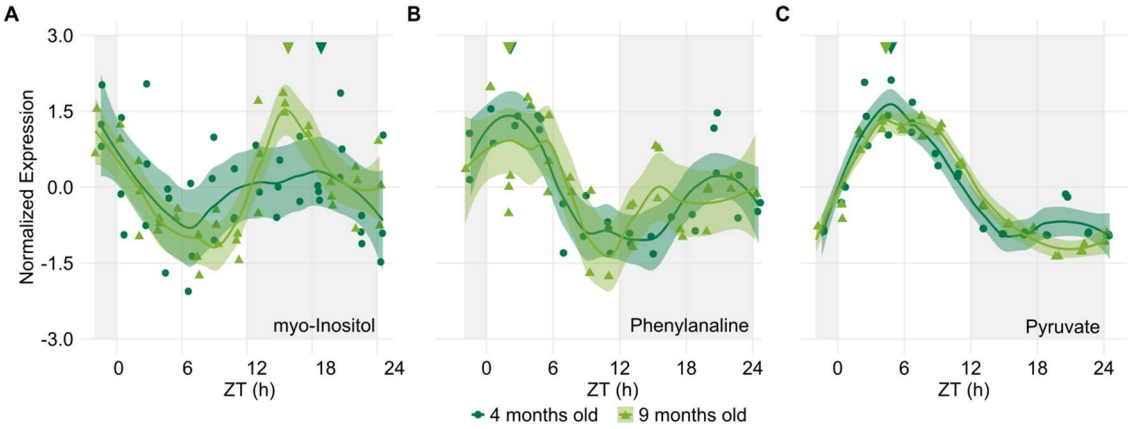

597

598 **Figure S3 – Metabolite rhythms that had an early phase or no phase change in 9**
599 **months old sugarcane compared to 4 months old sugarcane.** Leaf +1 of sugarcane
600 grown for 4 months old (4 mo., dark green) and 9 mo. (light green) in the field were
601 harvested for 26 h. Rhythms of (A) myo-Inositol, (B) Phenylalanine, (C) Pyruvate and (D)
602 Phenylalanine in 4 mo. and 9 mo. Metabolite levels were normalized with Z-score. All
603 biological replicates (circles in 4 mo. and triangles in 9 mo.) and their LOESS curve
604 (continuous lines ± SE) are shown. Inverted triangles show the time of the maximum value
605 of the LOESS curve. To compare the rhythms of samples harvested in different seasons,
606 the time of harvesting (ZT) was normalized to a photoperiod of 12 h day/ 12 h night. The
607 light-grey boxes represent the night period.

608

609 **Supplemental Figure 4**

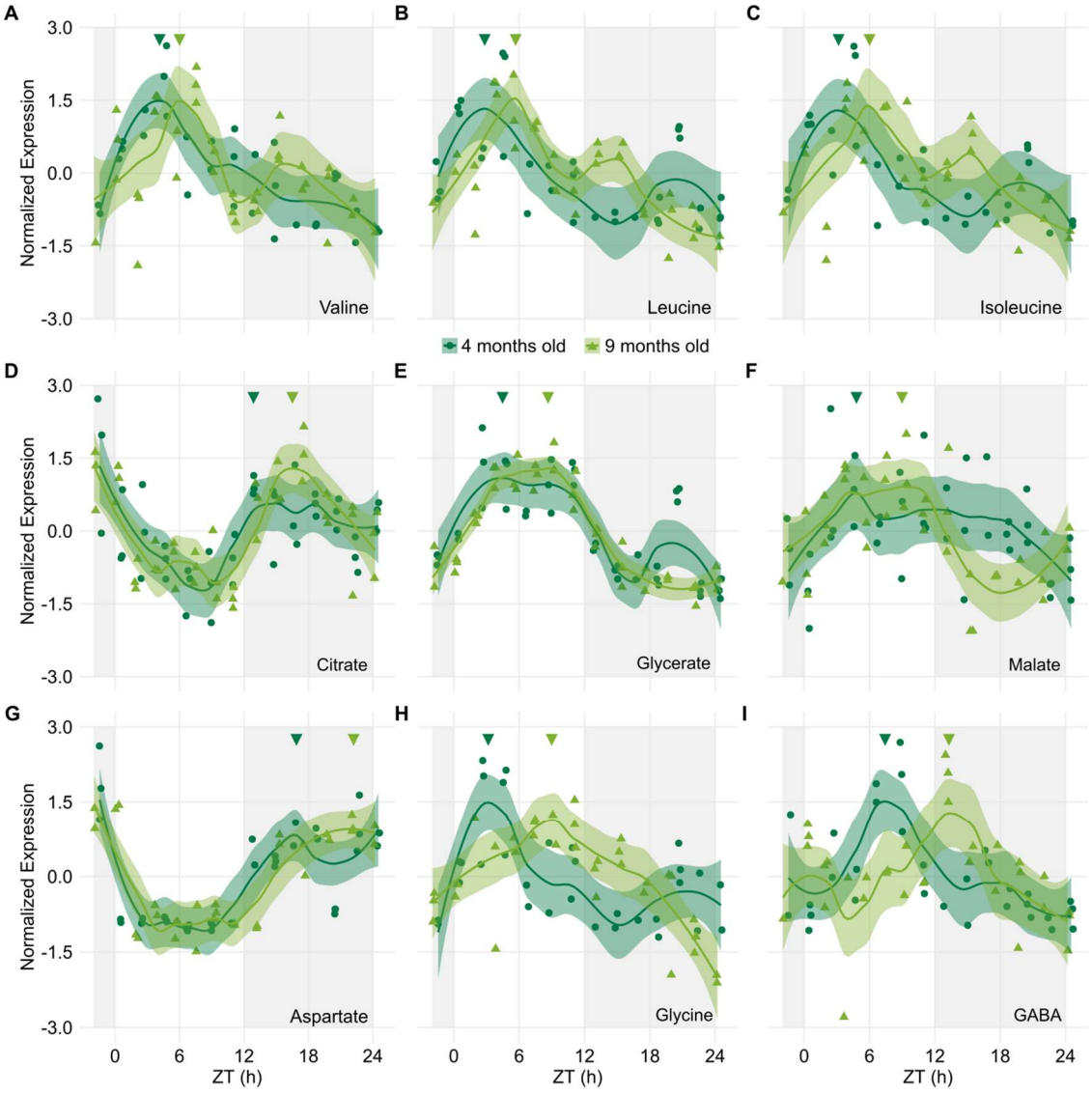

610

611 **Figure S4 – Metabolite rhythms that had a phase increase smaller or equivalent to 6**
612 **h in 9 months old sugarcane compared to 4 months old sugarcane.** Leaf +1 of
613 sugarcane grown for 4 months old (4 mo., dark green) and 9 mo. (light green) in the field
614 were harvested for 26 h. Rhythms of (A) Valine, (B) Leucine, (C) Isoleucine, (D) Citrate,
615 (E) Glycerate, (F) Malate, (G) Aspartate, (H) Glycine, and (I) GABA in 4 mo. and 9 mo.
616 sugarcane leaves. Metabolite levels were normalized with Z-score. All biological replicates
617 (circles in 4 mo. and triangles in 9 mo.) and their LOESS curve (continuous lines ± SE)
618 are shown. Inverted triangles show the time of the maximum value of the LOESS curve.
619 To compare the rhythms of samples harvested in different seasons, the time of harvesting
620 (ZT) was normalized to a photoperiod of 12 h day/ 12 h night. The light-grey boxes
621 represent the night period.

622 **Supplemental Figure 5**

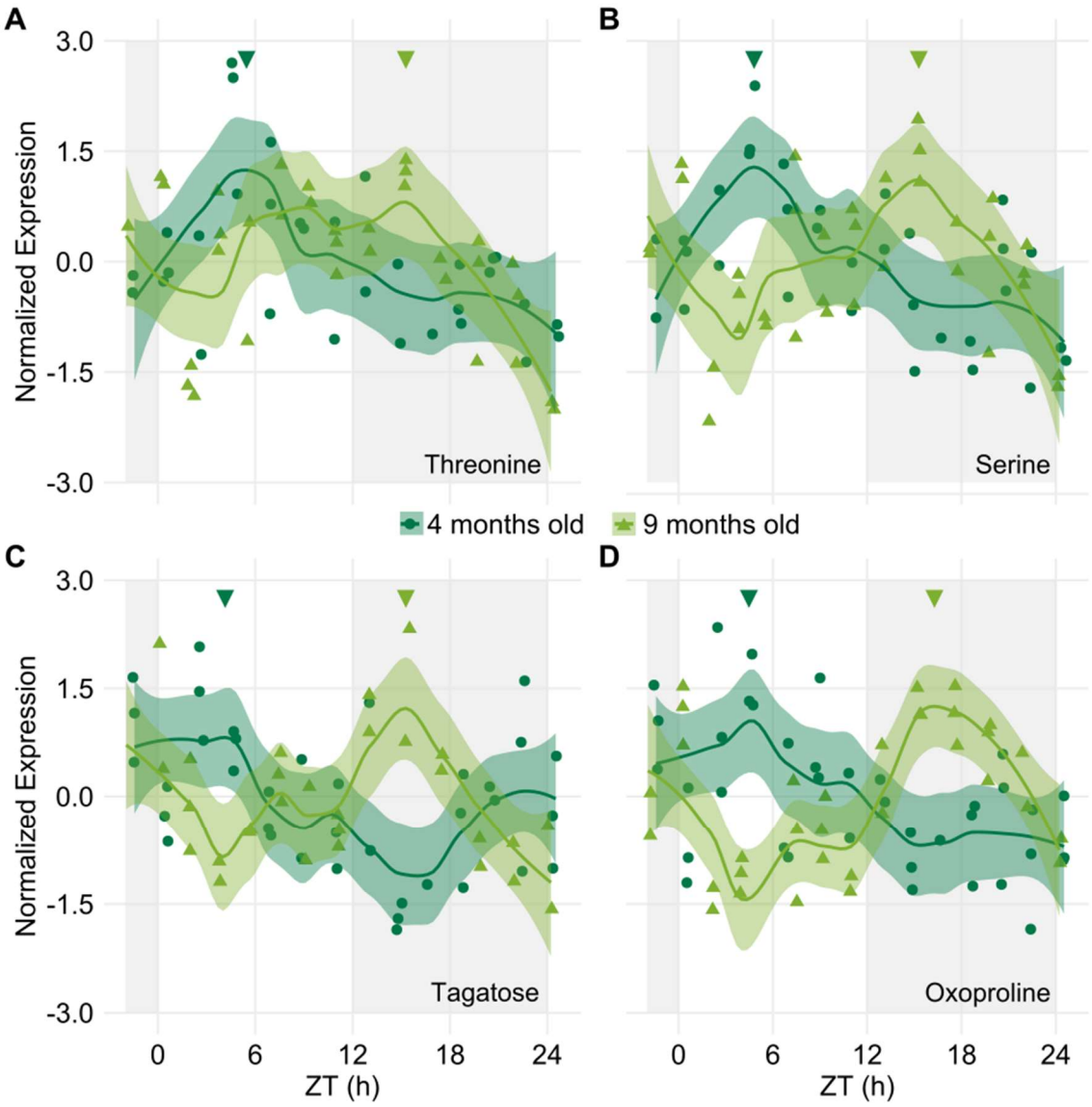

623

624 **Figure S5 – Metabolite rhythms that had a phase increase larger than 6 h in 9**
625 **months old sugarcane compared to 4 months old sugarcane.** Leaf +1 of sugarcane
626 grown for 4 months old (4 mo., dark green) and 9 mo. (light green) in the field were
627 harvested for 26 h. Rhythms of (A) Threonine, (B) Serine, (C) Tagatose and (D)
628 Oxoproline in 4 mo. and 9 mo. Metabolite levels were normalized with Z-score. All
629 biological replicates (circles in 4 mo. and triangles in 9 mo.) and their LOESS curve
630 (continuous lines ± SE) are shown. Inverted triangles show the time of the maximum value
631 of the LOESS curve. To compare the rhythms of samples harvested in different seasons,
632 the time of harvesting (ZT) was normalized to a photoperiod of 12 h day/ 12 h night. The
633 light-grey boxes represent the night period.

Supplemental Figure 6

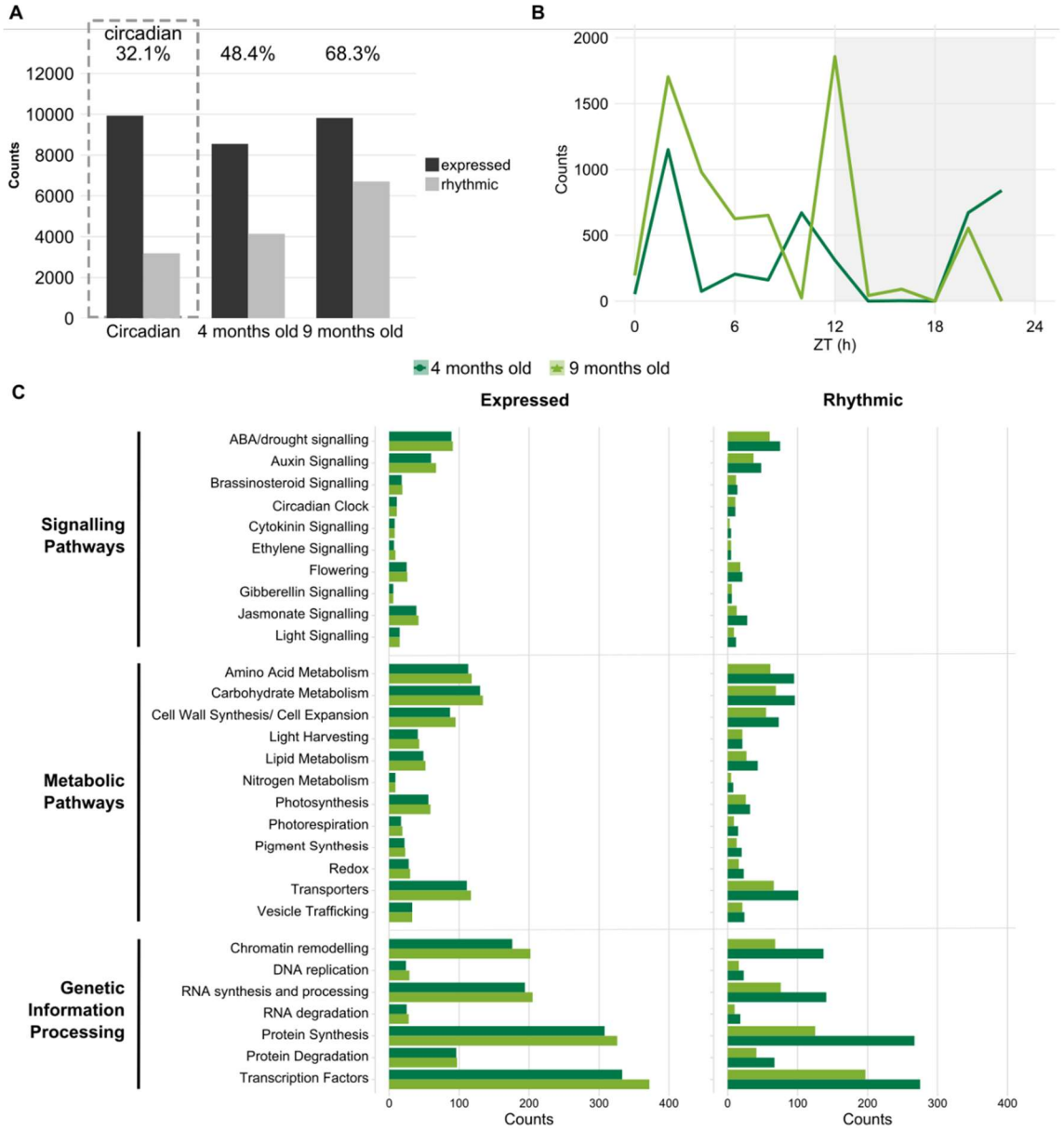

Figure S6 – 9 months old sugarcane has more rhythmic transcripts than 4 months old sugarcane. (A) The number of expressed and rhythmic transcripts detected in the leaves of 4 months old (4 mo.) and 9 mo. sugarcane in field-grown (diel) conditions, and in 3 mo. leaves in circadian conditions published in Hotta et al. (2013)(Hotta *et al.*, 2013). **(B)** Distribution of the peak time of rhythmic transcripts in 4 mo. and 9 mo. sugarcane. **(C)** Distribution of the functional categories of expressed and rhythmic transcripts in 4 mo. (dark green) and 9 mo. (light green) sugarcane.

644 **Supplemental Figure 7**

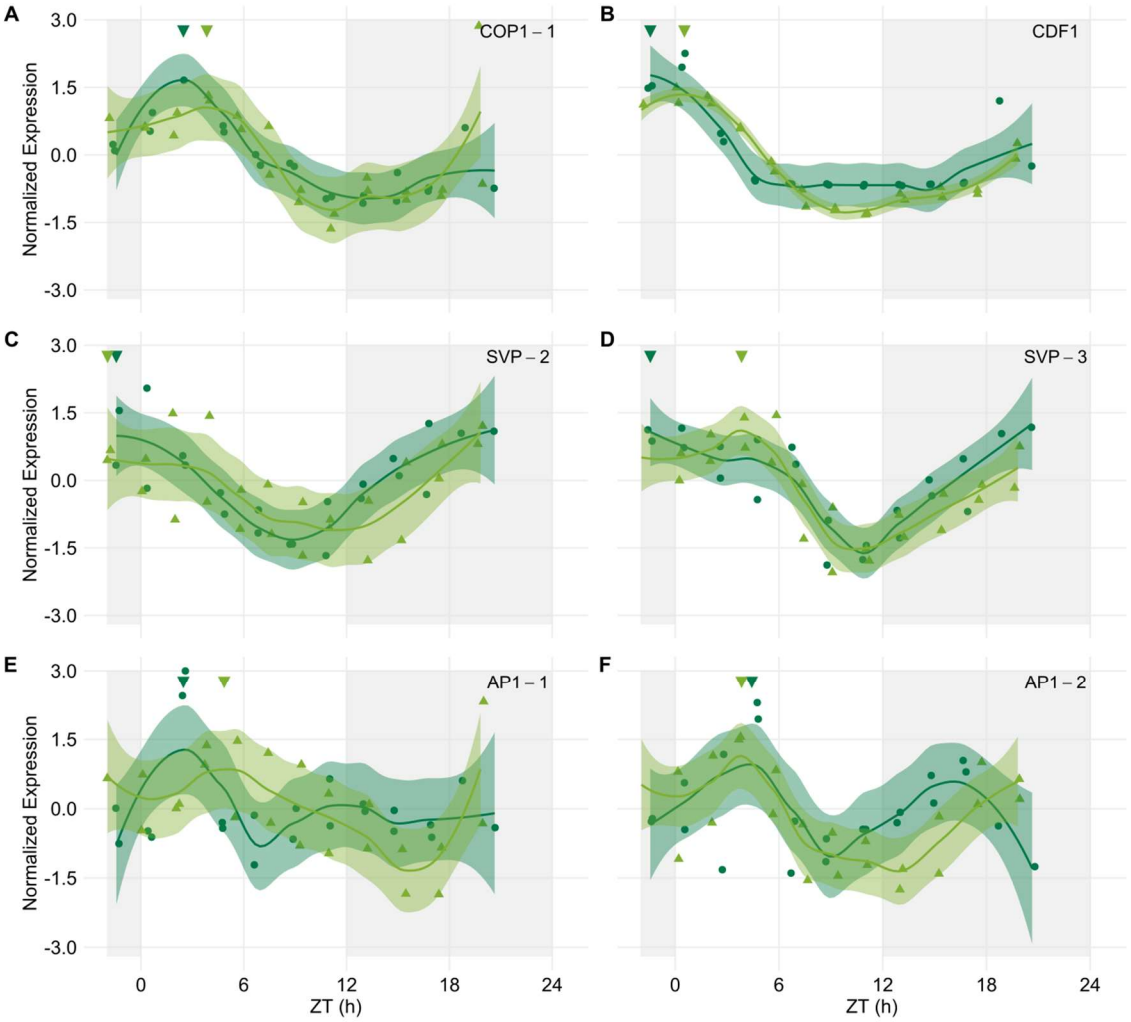

645

646 **Figure S7 – Rhythms of genes associated with flowering in the leaves of 4 months**
647 **old and 9 months old sugarcane.** Rhythms of (**A**) *CONSTITUTIVE*
648 *PHOTOMORPHOGENIC 1* (*ScCOP1*), (**B**) *CYCLING DOF FACTOR1* (*ScCDF1*), (**C**)
649 *SHORT VEGETATIVE-1* (*ScSVP*-2), (**D**) *ScSVP*-3, (**E**) *APETALA1*-1 (*ScAP1*-1), and (**F**)
650 *ScAP1*-2 were measured using custom Agilent oligo arrays in the leaves of 4 mo. and 9
651 mo. sugarcane grown in the field. All biological replicates and their LOESS curve
652 (continuous lines ± SE) are shown. Inverted triangles show the time of the maximum value
653 of the LOESS curve. Time series were normalized using Z-score. To compare the rhythms
654 of samples harvested in different seasons, the time of harvesting (ZT) was normalized to a
655 photoperiod of 12 h day/ 12 h night. The light-grey boxes represent the night periods.

656

Supplemental Figure 8

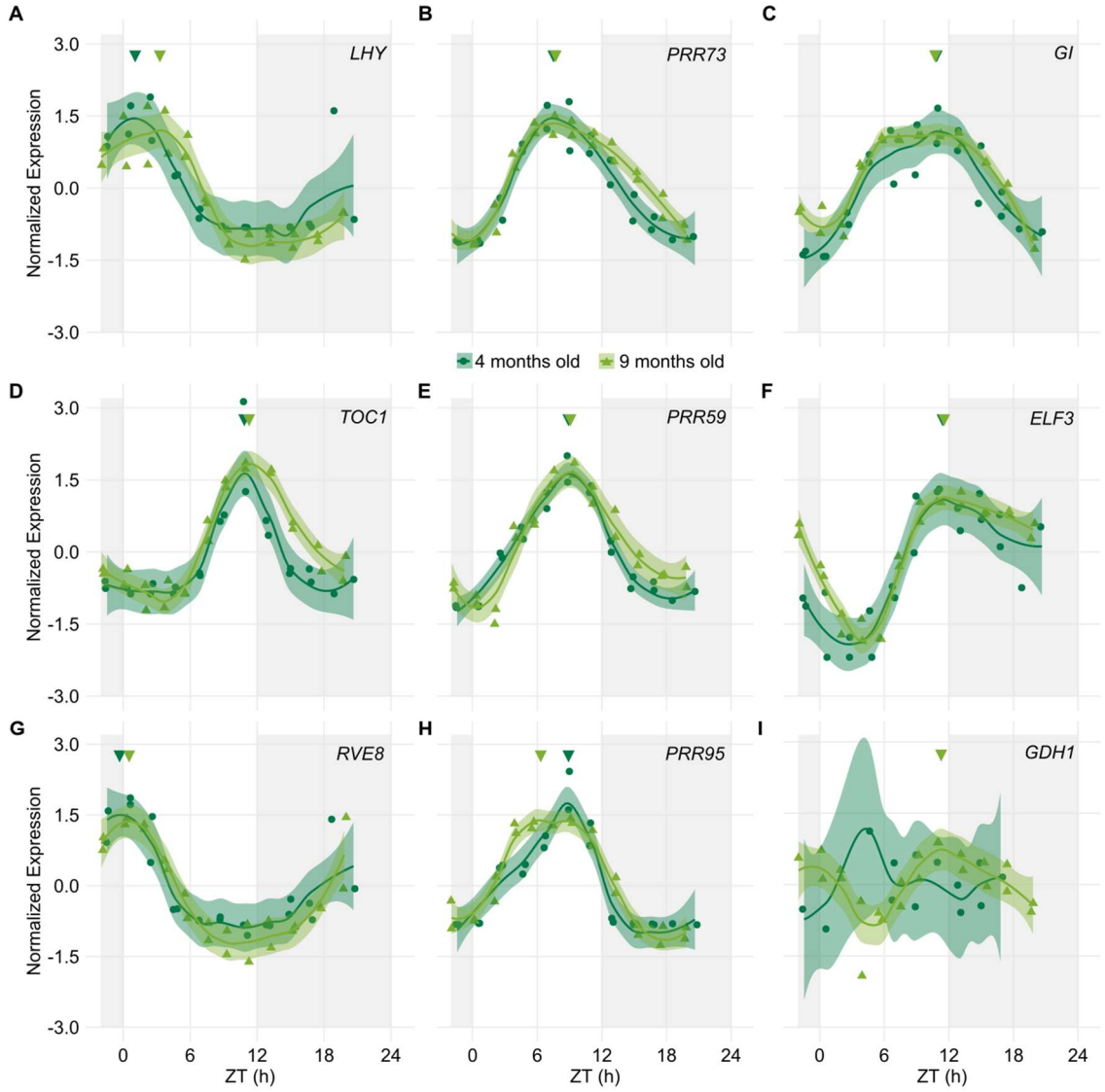

Figure S8 – Rhythms of circadian clock genes and N metabolism genes in the leaves of 4 months old and 9 months old sugarcane. Rhythms were measured using custom Agilent oligo arrays in the leaves of 4 mo. and 9 mo. sugarcane grown in the field. All biological replicates and their LOESS curve (continuous lines ± SE) are shown. Inverted triangles show the time of the maximum value of the LOESS curve. Time series were normalized using Z-score. To compare the rhythms of samples harvested in different seasons, the time of harvesting (ZT) was normalized to a photoperiod of 12 h day/ 12 h night. The light-grey boxes represent the night periods.

667 **Supplemental Figure 9**

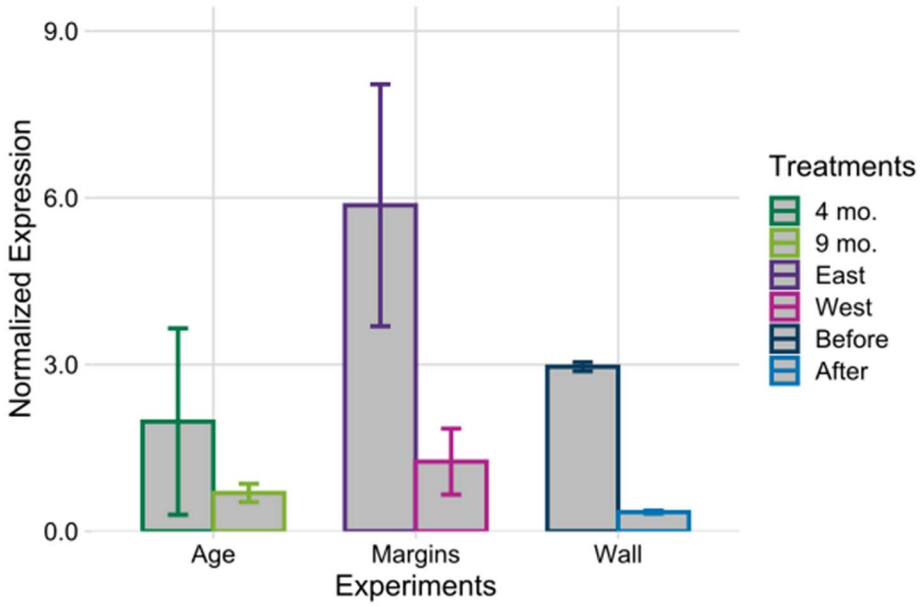

668

669 **Figure S9 – Transcript levels of *ScLHY* in the first hours of the morning.** In the Age
670 experiment, 4 months old (dark green) and 9 months old (light leaves) sugarcane leaves
671 were used. In the Margins experiment, sugarcane leaves from the East side (purple) or
672 the West side (pink) of the sugarcane field were taken. In the Wall experiment, sugarcane
673 leaves were taken from plants Before (dark blue) and After (light blue) a wooden wall on
674 the east side of the field. Sugarcane leaves were harvested between ZT0 and ZT2 (n=3).
675 Transcript levels were measured using RT-qPCR. Relative expression was determined
676 using *GLYCERALDEHYDE-3-PHOSPHATE DEHYDROGENASE* (*ScGAPDH*).

677

678 **Table S1 – Sugarcane genes and GenBank IDs**

Gene Symbol	Gene Name	SAS*	GenBank ID
AP1	*APETALA1*	SCQGLR1085G10.g	CA124279.1
CDF1	*CYCLING DOF FACTOR1*	SCMCCL6053D03.g	CA098046.1
COP1	*CONSTITUTIVE PHOTOMORPHOGENIC 1*	SCCCCL6003C08.g	CA096699.1
ELF3	*EARLY-FLOWERING 3*	SCEZLB1009F09.g	CA113166.1
FLD	*FLOWERING LOCUS D*	SCEQRT2090F09.g	CA138853.1
FT	*FLOWERING LOCUS T*	SCBFSD2035E11.g	CA278114.1
GAPDH	*GLYCERALDEHYDE-3-PHOSPHATE*	SCQGAM2027G09.g	CA086777.1
GI	*GIGANTEA*	SCJFAD1014B07.b	CA067312.1
LHY	*LATE ELONGATED HYPOCOTYL*	SCCCLR1048E10.g	CA167119.1
PRR59	*PSEUDO-RESPONSE REGULATOR 59*	SCACLR1057G02.g	CA116370.1
PRR73	*PSEUDO-RESPONSE REGULATOR 73*	SCACLR1057C07.g	CA116387.1
PRR95	*PSEUDO-RESPONSE REGULATOR 95*	SCCCLR1077F09.g	CA120437.1
RVE8	*REVEILLE 8*	SCSGST1070F10.g	CA179134.1
SVP-1	*SHORT VEGETATIVE-1*	SCCCLR1C05A05.g	CA189804.1
SVP-2	*SHORT VEGETATIVE-2*	SCCCLR1072F01.g	CA119595.1
SVP-3	*SHORT VEGETATIVE-3*	SCCCLR2001F11.g	CA127026.1
SOC1	*SUPPRESSOR OF CONSTANS OVEREXPRESSION*	SCCCLR2C03H07.g	CA127525.1
TOC1	*TIME OF CAB EXPRESSION 1*	SCCCSB1002H04.g	CA167119.1

679 * Sugarcane Assembled Sequence.

680

681 **Table S2 – Sugarcane primers pairs used to validate oligo arrays expression levels**
682 **using RT-qPCR**

Gene Symbol	SAS	Oligonucleotide sequence (5' -> 3')	Reference
GAPDH	SCQGAM2027G09.g	FWD CACGGCCACTGGAAGCA RVS TCCTCAGGGTTCCTGATGCC	Papini-Terzi et al. (2005)[a]
LHY	SCCCLR1048E10.g	FWD CCACCACGGCCTAAAAGAAA RVS TGGTTTTGTTGACTTGTCATTTGG	Hotta et al. (2011)b
TOC1	SCCCSB1002H04.g	FWD TTCTGCCTGAATTTGGCAAGTG RVS GGCATCGAGCACACCAATGC	Hotta et al. (2011)b

[a] Papini-Terzi et al. (2005) *DNA Research* 12:27, https://doi.org/10.1093/dnares/12.1.27

[b] Hotta et al. (2013) *PloS one* 8:e71847, https://doi.org/10.1371/journal.pone.0071847

683
684
685
686
687